NASA Contractor Report 185304

An Investigation into the Flow Behavior of a Single Phase Gas System and a Two Phase Gas/Liquid System in Normal Gravity with Nonuniform Heating from Above

Peter J. Disimile and Timothy J. Heist
University of Cincinnati
Cincinnati, Ohio

October 1990

Prepared for
Lewis Research Center
Under Grant NAG3-938

National Aeronautics and
Space Administration

Table of Contents

1.0 Introduction

The ignition and flame spread characteristics of liquid fuel pools are subjects of considerable scientific interest and are very relevant to fire safety applications such as aircraft crashes and petroleum spills. In many accident situations, including those which may occur in a space environment such as aboard an orbiting spacecraft, a flammable liquid is spilled in the vicinity of an ignition source such as hot engine parts or exhaust gases. Pool fires are complicated by multiple energy and mass transport processes, phase change, and chemical reaction.

In the presence of an ignition source, liquid motion is driven by both surface-tension gradients and liquid buoyancy[1]. These driving forces generally support in concert surface fluid motion away from the heat source. Therefore this motion tends to delay ignition as heat from the source is convected away rather than concentrated. On the other hand, the motion supports flame spread as the convection assists the preheating process ahead of the flame. The role of gravity varies depending on the relative strengths of buoyancy versus surface tension in driving the convection. If buoyancy contributes significantly, then a reduction in gravity will lead to more rapid ignition but slower flame spread. If surface tension gradients dominate, one might envision a longer ignition delay but a more rapid flame spread in reduced gravity. Theoretical studies in the literature 1,2,3 often assume that surface tension is the principal mechanism for motion of the liquid fuel ahead of the flame front for small laboratory scale experiments. However, Murad et al. 4 added a surfactant to a fuel which eliminated the temperature dependence of surface tension in the temperature range of interest. The effect of the surfactant was to reduce the ignition delay time, but to a much lesser extent than described above for the viscosity-enhanced fuel. They concluded that both forces, surface tension

and buoyancy, were important to the ignition problem. The authors did not isolate the effect of buoyancy in their experiments; experiments in reduced gravity allow such isolation to be accomplished. Recent theoretical studies [5,6] indicate that surface tension dominates only below a Grashof number of 104.

The importance of gas phase processes has not been treated quantitatively until recently [1,5,6]. While providing fresh oxidizer to a spreading flame, gas phase buoyancy in normal gravity was predicted to be very strong in the vicinity of the flame front. When the Grashof number was set equal to zero, the flame position shifted much closer to the liquid surface. This flame position shift is opposite that observed for solid surface burning in microgravity experiments [7]. In the solid surface case, the reduction in gravity moved the flame further from the solid surface presumably due to an inability of oxidizer to diffuse inwards in the absence of buoyancy. In the liquid pool burning case, however, liquid motion due to surface tension provides a possible convective mechanism for oxidizer to be entrained and brought close to the surface. If the flame resides closer to the surface, gas conduction, flame radiation, and the vaporization process differ from the case of normal gravity. Ignition delays will differ as well.

Before the effects of reduced gravity on liquid pool ignition and flame spread can be understood, these processes must first be fully examined in normal gravity conditions. As a first step, the fluid behavior of a single phase gas system and a two-phase gas/liquid system in an enclosed circular cylinder heated suddenly and nonuniformly from above was examined. Qualitative data on both systems was obtained using flow visualization. This data was used to define the system behavior in normal gravity conditions and to aid in the verification of a numerical model of the system [8].

2.0 The Experimental Apparatus

2.1 Single Phase Tests

The experimental setup used to determine the flow patterns is shown in Figures 1 and 2. The entire apparatus was constructed to be self-contained within the confines of a "drop rig" used in reduced gravity drop tower tests. This allows the identical experimental setup to be used in both normal and reduced gravity tests. The test cell was constructed from a cylindrical section of plexiglass and had a 0.4 cm wall thickness and was 10 cm in both height and diameter. In the center of the top surface (or end plate), a copper water-cooled jacket was employed to prevent this surface from melting and to simulate a concentrated heat source from above. The heater itself was fabricated from a thin nichrome wire encased in ceramic cement. All heaters used had a Type K thermocouple embedded in the center of the heater adjacent to the exposed heater surface. In this series of tests, 1.25 and 2.5 cm diameter ceramic heater were used. The radial temperature distribution of the heaters was checked using an infrared radiometer. Heaters which displayed a asymmetric temperature distribution were not used for the tests. In addition, the radial temperature distribution of a given heater can be deduced from the radiometric measurements and can be used to accurately model the heater in the numerical simulation. The flow was visualized by illuminating tracer particles in a single vertical plane by a light sheet created by a the beam of a 5 mW Helium-Neon laser through a cylindrical lens. The light sheet was reflected back across itself by a mirror to double the illumination. A B/W video camera was used to record the flow patterns on Fuji HQ VHS video tape. A heater temperature display and an experiment duration time display were placed in the field of view of the camera to record this information simultaneously with the flow field behavior. Tobacco smoke particles were

used as flow tracers. However, the tar in the tobacco smoke gradually began to coat the walls and bottom of the container. Over the course of approximately 20 test runs the walls of the test cell became too heavily coated to provide good flow visualization. The test cells were periodically cleaned ultrasonically in a water/alconox solution.

In an attempt to minimize the tar problem, the brand of cigarette used to produce the smoke was changed from Marlboro 100's to low tar Carlton's. For each test approximately 120 cc of smoke was injected into the test cell. This volume of smoke provided for adequate visualization when using the Marlboros whereas the much less opaque smoke of the Carltons reduced the quality of the visual image. The smoke was injected slowly (at a rate of 10 cc every 15 seconds) to reduce the waiting time for the motion of the injected smoke to damp out. A waiting time of 4 minutes provided the best results. The test was then initiated by powering the laser and video camera, followed by the heater and cooling pump. In some runs, the heater was brought up to its steady state temperature outside the test cell, then gently put into place, initiating the start the test.

2.2 Two-Phase Tests

The experimental setup used in the two-phase tests was very similar to the single phase tests. Additional cells fabricated from clear arcylic blocks and tubing measuring 10 cm high x 5 cm diameter, and 5 cm x 5 cm were used for the two-phase tests. A square test cell 5 cm high with a 4.2 cm hole bored through the center was used to provide better observation of the liquid phase by eliminating the refractive error. In addition to the 1.25 and 2.5 cm heaters used for the single phase tests, a 1.75 cm heater was also used. Two miniature, high resolution Pulnix B/W video cameras with macro lenses provided simultaneous views of the entire test cell and the gas-liquid interface. On several occasions a 35 mm still camera was used for

long time-exposure pictures, ranging from 10 sec. to 2 min., of the liquid phase to help establish the predominant flow pattern. Most of the two-phase data was taken for a liquid fill level of 50% of the test cell height with 10 centistoke silicone oil as the test liquid. Density-matched 12 μm plastic particles traced the flow in the liquid phase. When a gas phase tracer was required, tobacco smoke was again used. The major disadvantage of using the tobacco smoke was the resulting settling of the smoke into the liquid, which eventually made the liquid too opaque for adequate visualization and could have potentially caused changes in its surface tension. However, the use of the tobacco smoke provided additional flow visualization in the liquid phase. As a test progressed, the smoke particles gradually became entrained in the liquid and provided a clear outline of the flow pattern.

2.3 Flow Visualization Using Liquid Crystals

With the exception of qualitative flow visualization data, no other useful data was collected for the two-phase system. The problems encountered with determining velocity gradients in the liquid phase are discussed below with the results of the two-phase tests. A problem that is perhaps more important than resolving the velocity vectors is determining temperature gradients in the liquid phase. This problem prompted an investigation into the feasibility of using microencapsulated liquid crystal particles to seed the flow, thus allowing for the simultaneous collection of both flow pattern and temperature gradient data. To determine in which manner the liquid crystals could be used to obtained the desired qualitative and quantitative information, several variations of the same experimental setup were used. These variations are shown in Figure 6 and are described with the test results. The basic experimental setup was as follows. The 5 cm x 5 cm square test cell was positioned so that a vertical sheet of white light passed through the center of the test cell. A heater and cooling jacket is

placed at the top of the test cell. A Nikon F3 35 mm still camera recorded the position and color of the liquid crystal particles over a given period of time as they move with the flow.

The most critical part of the experimental setup was the creation of the light sheet. The ideal light source was one that would not induce any motion in the liquid pool due to radiation from the visible or infrared range of the spectrum. Thus, the major problem encountered was one of finding a light source which will provide adequate illumination of the pool while not disturbing the flow. The two light sources tested were an incandescent 6 volt, 18 amp oscilliscope bulb, and a xenon arc strobotach.

Each test was performed in the following manner. The test cell was filled to 50% of its height with a mixture of distilled water and liquid crystal concentrate (water heavily seeded with liquid crystal particles). The microencapsulated liquid crystal particles were mostly in the 10-15 μm diameter range with a red color start of 30 °C and blue start at 42 °C. Over a period of time the particles would begin to settle to the bottom of the test cell, therefore, 30 minutes prior to each test the particles are redistributed in the pool by drawing 30-40 cc of the water in the pool into a syringe and injecting it back into the pool. This was more effective than simple stirring. This was done 30 minutes prior to a test so that the motion induced from the injection was damped out. To minimize any flow induced by the light sheet, the light source remained off until the start of the test. The heater is brought to a steady temperature before it was put in the test cell. The resulting flow patterns and temperature gradients were recorded on color slide and print film using various exposure times. Throughout these tests a number of different types and speeds of film were evaluated. Overall, the film that provided the results was Kodak Kodacolor 400. The high light sensitivity produced adequate pictures in low light conditions while still having fine enough grain to preserve some of the details of the flow patterns and temperature gradients. Higher speed films

such as ASA 1000 and 3200 were also tested but were found to have much too coarse of a grain for quality pictures under these lighting conditions.

Slide film was also used in some tests. The greatest advantage of slide film are color preservation and for data analysis as the slides could be projected onto a large screen or more easily image processed. The two types of slide film used were Ekatachrome 400 and AFGA 1000. The Ektachrome gave very poor results, i.e. no color preservation, while the 1000 speed film did produce some mild improvement.

3.0 Results and Discussion

3.1 Single-Phase Tests

The first series of single phase tests were performed using a 1.25 cm heater at temperatures between 353 K and 836 K. These temperatures signify the centerline temperature near the heater surface. The flow patterns that were observed at various temperatures were ultimately grouped into three series of flow patterns that correspond to three ranges of heater temperatures. Regardless of heater temperature, the initial flow behavior observed was the formation of a single toroidal vortex in the upper region of the test cell. Since only a vertical cross section of the test cell is being viewed, this toroidal vortex appears essentially as two vortical "cells", one on either side on the test cell. In all cases this flow pattern was observed to be very symmetric in nature. For heater temperatures ranging from 767 K to 836 K, the initial flow pattern evolved into an asymmetric flow pattern characterized by the formation of "figure-eight" vortical arrangement in the right hand side of the test cell (w.r.t. its axis of symmetry) and a single elongated vortex in the left half on the test cell. The "figure-eight" arrangement is characterized by the formation of an additional vortical cell in the lower portion of the test cell. This

secondary vortex is both smaller and weaker than the upper cell. These flow patterns evolved after approximately 7 minutes of run time.

In the 610 K to 705 K range, fluid behavior was characterized by the development of the same initial flow pattern followed by, approximately 50% of the time, the formation of symmetric lower cells having a slower rotational speed than the upper cells. When observed, these lower cells formed after approximately 1.5 minutes of run time and did not appear to evolve from the growth of the upper cells. This flow pattern was attributed to the radiative heat transfer between the heater and the bottom plate of the test cell. However, as run time increased the lower cells seem to be overcome by the upper cells which become increasingly elongated and extend towards the base of the test cell.

For heater temperatures between 353 K and 550 K the initial flow pattern remained symmetric and extended downward to a position approximately one half of the test cell height and appeared to reach a steady state configuration. This was the only flow pattern observed after 8 minutes of run time.

The results of this first series of single phase tests led to a modified experimental test matrix for the next series of tests. The remaining single phase tests concentrate on defining the flow pattern behavior at or near heater temperatures of 550 K, 670 K, and 820 K. In this series of tests a new 1.25 cm heater and a 2.5 cm heater of the same construction were also used.

This series of tests revealed the set of specific flow patterns, observed after approximately 8 minutes of run time, for each temperature and heater size, as shown in Figure 3. Regardless of heater temperature or size, the progression of the flow pattern development began with the initial roll up and growth of a symmetric toroidal vortex described above. This vortex continues to grow and elongate before evolving into another flow pattern.

For the 1.25 cm heater at temperatures near 550 K the only flow pattern observed is shown in Figure 3a. The vortex grew to a point where it extended approximately three-quarters of the way down in the test cell and remained at this level for the duration of the run. When the heater temperature was increased to 670 K, the initial flow pattern reached the bottom of the test cell. Within the vortex, a saddle point formed approximately one-third of the way up from the bottom of test cell (see Figure 3b). It appeared as though a second vortex was about to form in the lower portion of the test cell, but at this heater temperature the lower vortex never formed. At a heater temperature near 820 K the flow pattern development initially progressed much the same as it did for the 670 K heater temperature. As the run time increased, a lower vortex was generated near the bottom of the test cell (Figure 3c). This secondary vortex was considerably smaller and rotated at a much slower rate than the upper, primary vortex.

Several differences in the steady state flow patterns were observed when the 1.25 cm heater was replaced with the 2.5 cm heater. At 550 K, the upper vortex developed in the same manner described above, but extended to the bottom of the test cell (Figure 3d). For heater temperatures near 670K, a weak, symmetric lower vortex formed as the run progressed (Figure 3e). This flow pattern was never observed using the smaller heater at this temperature. At 820 K, the fluid behavior was much the same as with the small heater at the same temperature, but the lower vortex that developed was slightly larger and appeared to be rotating at a faster rate (Figure 3f).

In addition to these results, some more general observations were also made. The symmetry of the radial temperature profile of the heater had a pronounced effect on the symmetry of the toroidal vortices. When a heater with an asymmetric temperature profile was used, an asymmetry in the flow

pattern was observed. When this heater was rotated 180°, the flow pattern asymmetry appeared on the opposite side of the test cell.

Over the course of several runs, the exposed surface of the heater was gradually covered with the tar from the tobacco smoke. Throughout the course of this series of tests, both clean and coated heaters were used with no noticeable differences between the observed flow patterns at any temperature. Tests with an infrared radiometer also suggested that the emissivity of the heater surface was near unity even before any exposure to the tobacco smoke.

3.2 Two-Phase Tests

The first series of tests were performed with the 10 cm x 5 cm cell and the 1.25 cm heater at temperatures of 340, 550, 670, and 820 K. In these initial tests it was desired to only observe the motion in the liquid phase, therefore no gas phase tracer was used.

At a heater temperature of 340 K there was no noticeable change in the motion of the liquid from the initial conditions. At 550 K, there was flow at the gas-liquid interface from the center of the pool toward the wall of the test cell, but the flow down the wall and back toward the center was not easily observed. The fluid velocity below the liquid surface was too slow to observe without time lapse photographs. However, as the run progressed, dark streaks outlining the required toroidal vortex begin to appear. These dark streaks were regions where the tracer particles were no longer present.

At heater temperatures of 670 and 820 K there was a noticeable increase in the liquid velocity at the interface and in the velocity of the return motion. While this increase in the vortex strength was clearly evident, the magnitude of the velocity vector was still very small. Measuring the displacement of individual tracer particles over a given period of time to determine the fluid velocity proved impossible. There was no visually

detectable difference in the fluid velocities at or below the interface between the 670 and 820 K runs.

The first series of tests were repeated with the 2.5 cm and 1.75 cm heaters. For the 2.5 cm heater, the motion in the liquid phase was nearly identical to that observed using the 1.25 cm heater with the exception that there appeared to be a slight increase in fluid velocity at comparable heater temperatures, based on visual observations.

The fluid velocities observed when using the 1.75 cm heater, while still relatively slow, were greater those observed at comparable temperatures using the 2.5 cm heater. This is most likely attributable to the difference in radial temperature distributions caused by differences in the physical construction of the heaters. The 1.75 cm heater was constructed by spiralling the nichrome wire heating element whereas the 2.5 cm heater had a snowflake shaped wire pattern. The spiral wire design had more heated wire per unit surface area, most likely resulting in a higher average surface temperature for the same centerline temperature. Unfortunately, the radiometer was not available to determine the radial temperature of the 1.75 cm heater, thus the hypotheses could not be confirmed. It should also be noted that the 1.75 cm heater reaches its steady state, centerline temperature in approximately 2-3 minutes whereas the other heaters required around 6 minutes.

Investigation of the gas phase of this system showed three distinct flow patterns corresponding to the 550, 670, and 820 K heater temperatures. For a given heater temperature, there was very little difference in the observed gas phase flow pattern for each heater size. Both the gas and liquid phase flow patterns are shown in Figure 4a,b,c.

The next series of tests were done with the 5 cm x 5 cm test cell and the 1.75 cm heater at the same temperatures mentioned above. The other two heaters were not used since there appeared to be very little dependence on heater diameter over the tested temperature range. Several runs were done

with the square test cell described above. This test cell provided excellent visualization of the liquid phase but the gas phase was very distorted due to the refractive index mismatch of the cell and the air. With the round test cell the opposite occurs, therefore both test cell were used to determine the behavior of the liquid and gas phase.

The flow patterns shown in Figure 4d,e,f are a culmination of test results from both 5 cm x 5 cm test cells. Surprisingly, in all of the tests, there were no significant differences in the gas-phase flow patterns for each heater temperature. Liquid-phase flow patterns differed only slightly between temperatures, with the visible vorticies extending closer to the center of the pool with increasing heater temperature, just as they did in the 10 cm x 5 cm cell tests.

Several tests were conducted using the 10 cm x 10 cm test cell. These tests showed that at a fill level of 50%, the resulting flow patterns are identical to those observed for the 5 cm x 5 cm test cell. This is the expected result for test cells with identical H/D (height/diameter) ratios and fill levels.

3.3 Liquid Crystal Evaluation Tests

The first set of tests were conducted using the experimental setup shown in Figures 5a and 5b. In this setup, the incandescent lamp operating at 6 volts, 15 amps, and a video camera lens to focus the filament of the lamp vertically of the side of the test cell to provide a light sheet. It became immediately obvious by visual inspection that the radiation from the lamp induced motion in the pool prior to introducing the heater. In an attempt to reduce the effect of the lamp, several changes were made during this first series of tests. Among them were the addition of an infrared filter and a heat trap in the form of a plastic box filled with water through which the light passed before reaching the test cell. In order to

reduce the thickness of the light sheet, the video lens was removed and a cylindrical lens and a 3 mm slit were placed on the side of the test cell.

The observations made during these tests were encouraging. The liquid crystal particles were large enough to make both the flow due to heater and the light source clearly visible. The fluid temperature was represented by a color band, blue to red, that started at the center of the pool, spread out the walls of the test cell then propagated deeper into the pool as the run progressed. The high degree of the color saturation on the photographs of these initial runs was due to the high seeding density of the liquid crystal particles. Unfortunately, none of the adjustments made to the experimental setup eliminated the effects of the light source. A few more tests were conducted using the initial configuration with the incandescent lamp to evaluate the usefulness of intermittently blocking the light while exposing the film. It was found that this method did not help to reduce the effects of the lamp on the flow.

Since the flow induced by the light source was very asymmetric, during the next series of tests the lamp was placed approximately 6 inches directly below the test cell, bringing the light sheet in from the bottom (see Figure 5c). By doing this the induced flow was much more symmetric with a single vortical cell on both sides of the test cell.

Variations of this setup included the heat trap and a fan to convect some of the heat away from the lamp. Even with these changes, the light-induced motion remained. However, immediate reduction in this motion was observed when the heater was inserted. While the light-induced motion was not completely dissipated, the size of the vorticies shrank throughout the run.

Having realized that the problems encountered with the incandescent lamp could not be easily resolved, it was decided to try an alternate light source. A xenon arc strobotach was chosen since the infrared emission was lower and the variable flash rate could be used to illuminate the test cell

at a selected frequency. It was hoped that this would reduce the lighting effects while still providing adequate illumination for flow visualization. The strobotach was positioned such that the light passed through an infrared filter and a large slit before reaching the cylindrical lens and a 2mm slit on the side of the test cell (see Figure 5d). The initial flash rate was set at 110 flashes/min.

Several runs were conducted using this setup. While there was still some motion induced by the light, visual inspection seemed to indicate that it was not as severe as with the incandescent lamp. The flow patterns observed were similar to those seen in previous runs.

The particle seeding density was then lowered (1cc concentrate mixture) to where individual particles could be tracked stroboscopically, i.e. the color play of an individual particle could be observed over time. The major disadvantage of using a low seeding density is that there was much less light reflected from the particles, making it more difficult to photograph them.

A special flat-topped xenon arc bulb was located for the strobotach that provided for improved illumination by focusing the filament on only the lower half of the test cell (see Figure 5e). In addition to the new bulb, a mirror was placed on the opposite side of the test cell to increase the illumination. Some runs using this configuration were conducted using a higher seeding density, in these runs a 4 cc concentrate mixture was used. With the exception of some of the very high seeding density tests, the combination of the 4 cc mixture and the lighting configuration described above seemed to produce the best results.

The strobotach was next placed beneath the test cell to determine if its effectiveness could be improved in this configuration (see Figure 5f). These tests gave results comparable to the previous strobotach setup. No improvement was noted when the particle seeding density was increased to a 10 cc concentrate mixture.

The final experiment configuration involved lighting from beneath the test cell with the incandescent lamp, but now the lamp was not positioned directly beneath the test cell rather it was offset to one side (see figure 5g). The light was reflected up to the test cell with a surface coated mirror. The purpose of arranging the illumination components in this manner was to eliminate the effects due to heat convecting up from the lamp. However, this configuration did not offer any improvements over previous tests.

One important point to note concerning these tests is that even though the infrared filter was placed in front of the light source in many tests, it did not seem to have any effect on reducing the flow induced by the light source. This supports the theory that the motion is actually caused by the liquid crystal particles absorbing visible radiation, heating up, and causing buoyant flow. The most promising idea yet to be evaluated is the concept of introducing the light sheet downward from above the test cell. This should help eliminate the effects of the light source since the hottest particles would be resident on the top and the pool would be stratified.

4.0 Summary

The fluid behavior of a single phase gas system and a two-phase gas/liquid system enclosed in an circular cylinder nonuniformly heated from above, under normal gravity conditions has been investigated. These studies were carried out for test cells of various sizes and H/D (height/diameter) ratios using three different diameter heaters. A direct injection/laser light sheet flow visualization technique was used to obtain qualitative data on both systems. The results of the single phase and two-phase tests under normal gravity conditions can be used to more fully understand the behavior of such systems in a reduced gravity environment. Single phase system tests performed with a 10 cm x 10 cm test cell showed that the observed flow

patterns were a function of both heater size and temperature. Distinct steps in the progression of the flow patterns from a single toroidal vortex to a two-cell configuration are observed at heater temperatures near 550 K, 670 K, and 820 K. The transition to the two-cell configuration was observed to occur at a lower temperature as the diameter of the heater was increased.

The two-phase system was examined for test cells having H/D = 1 and H/D = 2 which correspond to test cell dimensions of 5 cm x 5 cm and 10 cm x 5 cm respectively. A liquid fill level of 50% of the test cell height was used for all tests. The observed gas phase and liquid phase flow patterns appeared to only be a function of heater temperature for each test cell.

An attempt was made to use thermochromatic liquid crystal particles as flow tracers in the liquid phase of the system. This would have facilitated the simultaneous gathering of both flow pattern and temperature gradient data. Several different experimental configurations were used to determine feasibility of this concept and the most appropriate method of creating a light sheet which would not disturb the system. From these tests is was determined that introducing the light sheet from above the test cell would most likely provide the best results. This approach has yet to be explored in detail.

5.0 References

1. Furuta, M., Humphrey, J.A.C., and Fernandez-Pello, A.C., "Prediction of Flame Spread Hydrodynamics Over Liquid Fuel," Physico-Chemical Hydrodynamics , Vol. 6, No. 4, 1985, pp. 347-372.

2. Glassman, I. and Dryer, F.L., "Flame Spread Across Liquid Fuels," Fire Safety Journal , Vol. 3 1980/1981, pp 123-138.

3. Sirignano, W.A. and Glassman, I., "Flame Spreading Above Liquid Fuels: Surface-Tension-Driven Flows," Comb. Sci. Tech., Vol. 1, 1970, pp. 307-312.

4. Murad, R.J., Lamendola, J., Isoda, H., and Summerfield, M., "A Study of Some Factors Influencing the Ignition of a Liquid Fuel Pool," Combustion and Flame, Vol. 15, 1970, pp. 289-298.

5. Aggarwal, S.K., Iyengar, J., and Sirignano, W.A., "Enclosed Gas and Liquid with Nonuniform Heating from Above," Int. J. Heat Mass Transfer, Vol. 29, 1986, pp. 1593-1604.

6. Abramzon, B., Edwards, D.K., and Sirignano, W.A., "Transient, Stratified, Enclosed Gas and Liquid Behavior with Concentrated Heating from Above," J. Thermophysics, Vol. 1, No. 4, October 1987, pp. 355-364.

7. Altenkirch, R., and Vedha-Nayagam, M., Paper 3-D2, 1986 Spring Technical Meeting, Central States Section; The Combustion Institute.

8. Ross, H.D., Schiller, D.N., Disimile, P., and Sirignano, W.A., "Behavior in Normal and Reduced Gravity of an Enclosed Liqid/Gas System with Nonuniform Heating from Above," NASA Technical Memorandum 101471, AIAA-89-0070, prepared for the 27th Aerospace Sciences Meeting, January 1989.

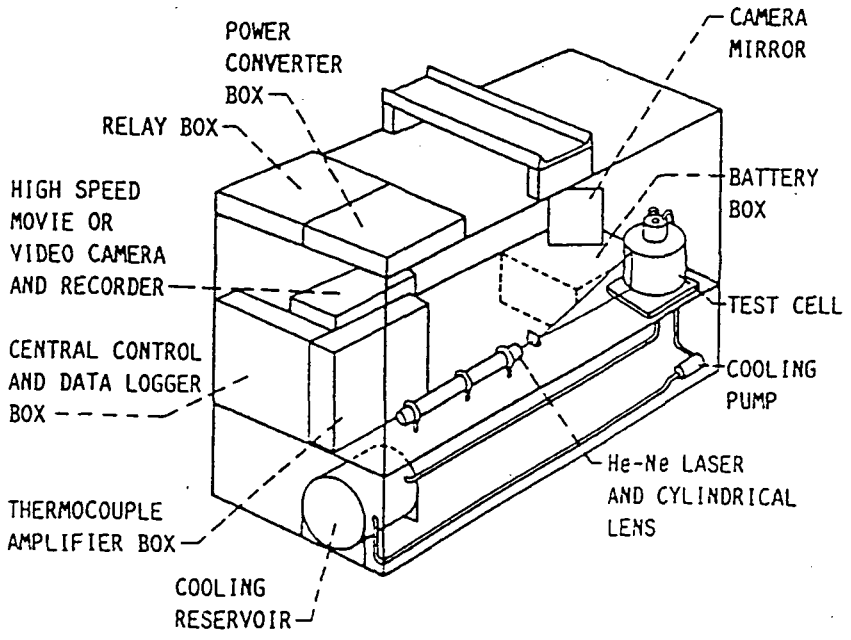

Figure 1: Arrangement of experimental apparatus in "drop rig" for future use in reduced gravity tests.

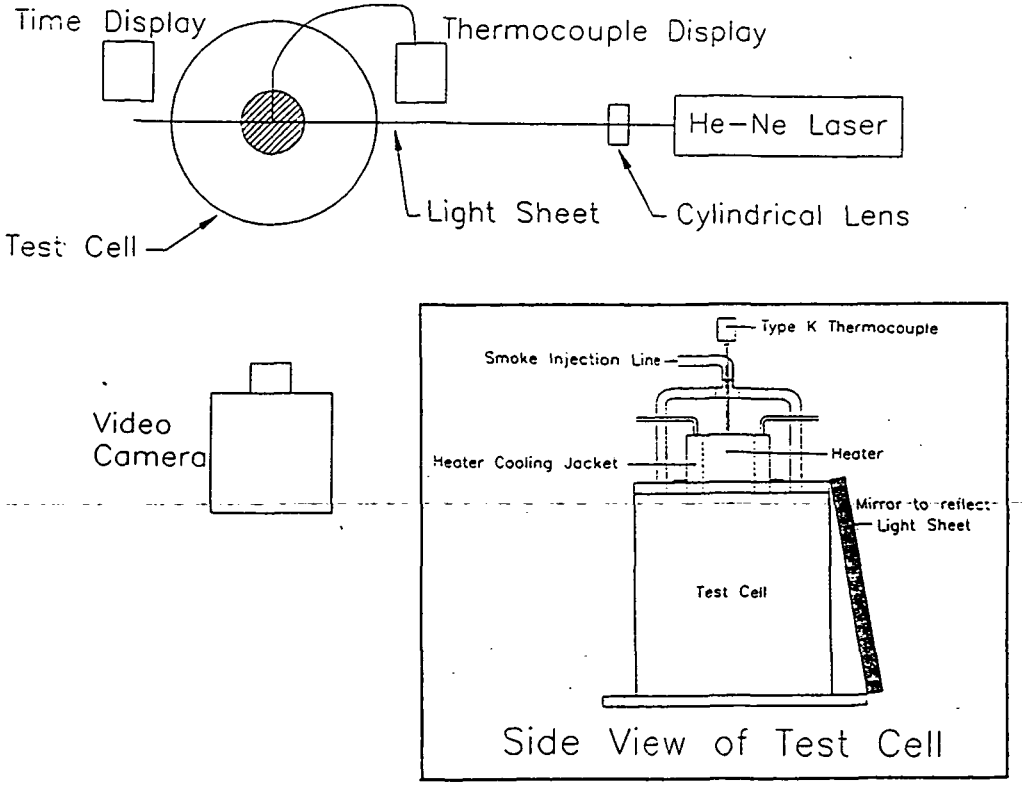

Figure 2: Experiment and test cell configurations.

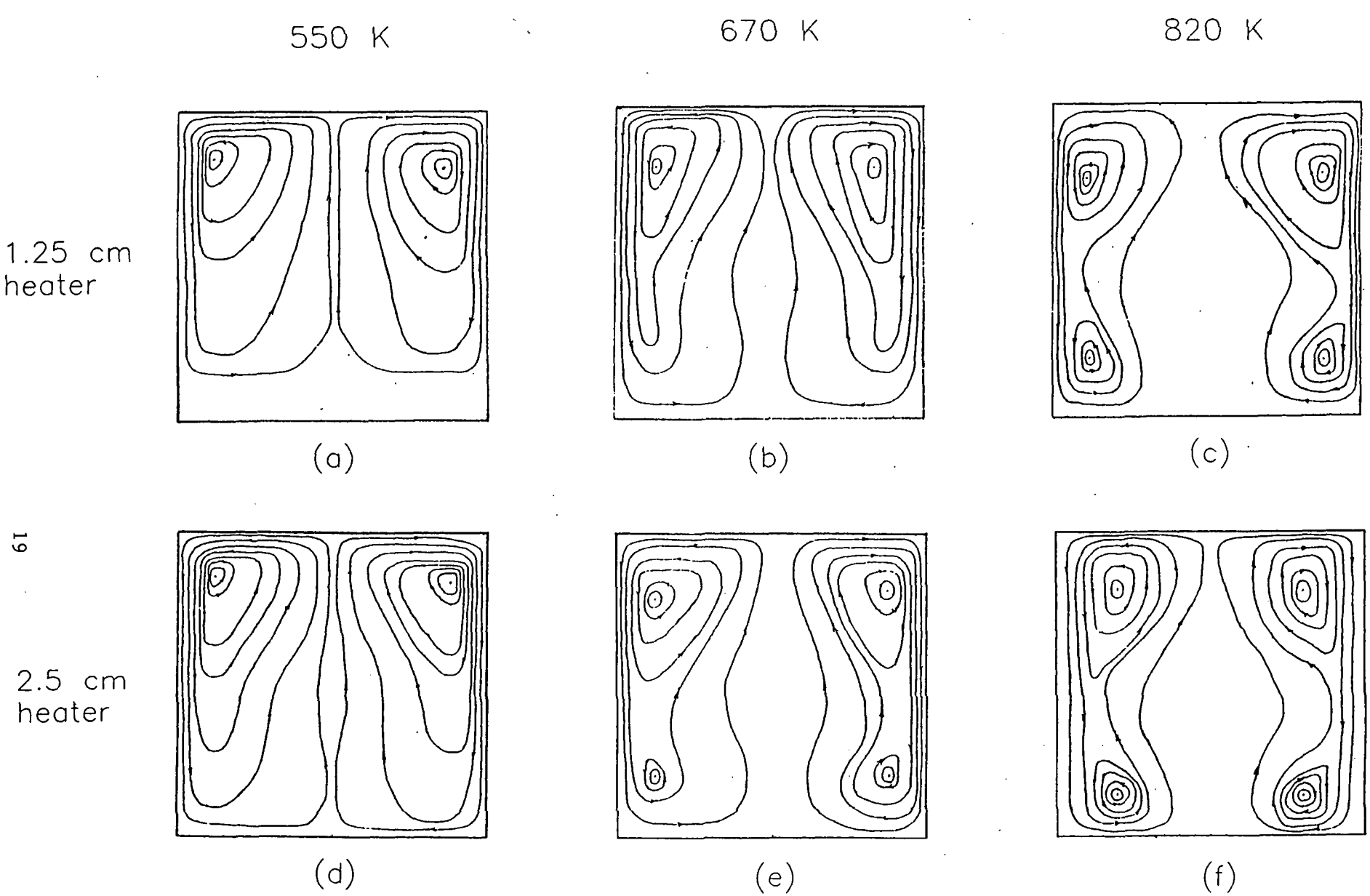

Figure 3: Single–phase flow patterns as function of heater size and temperature

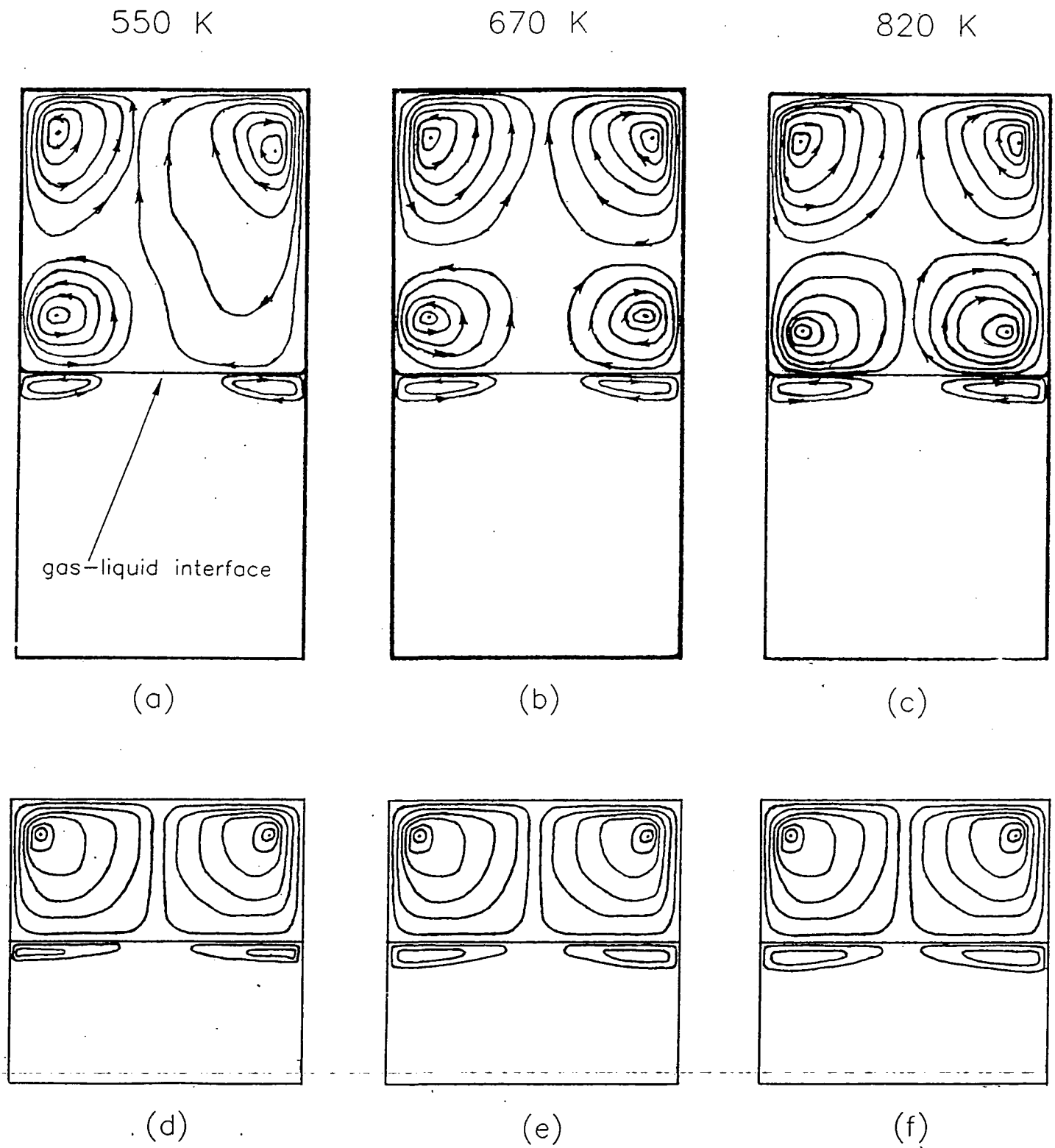

Figure 4: Two–phase flow patterns as a function of heater temperature.

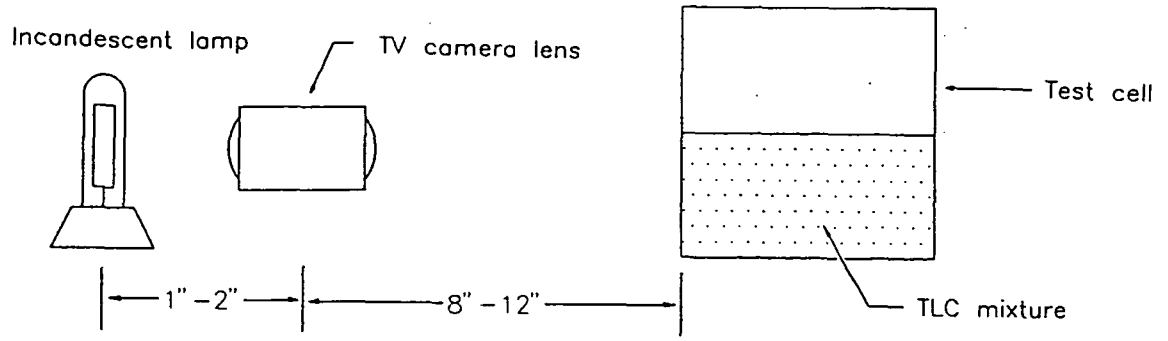

(a)

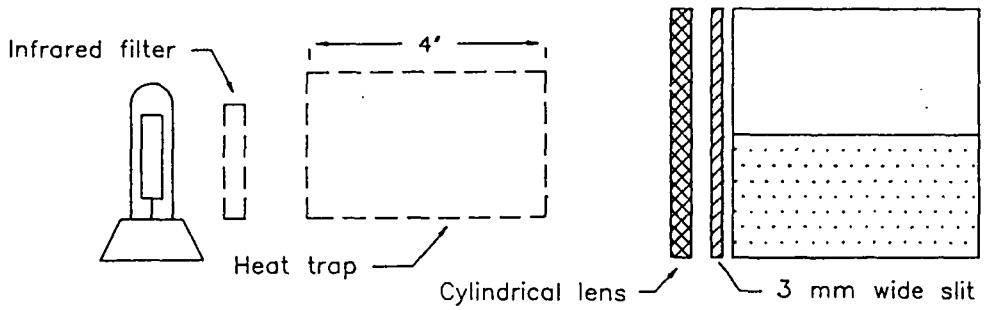

(b)

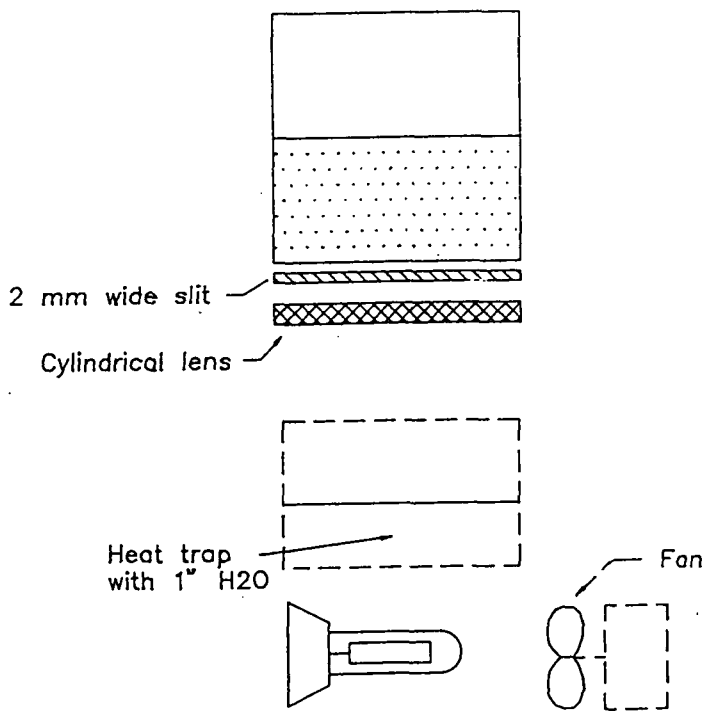

(c)

NOTE: Dashed lines indicate that the given apparatus was not used in all tests performed with that set-up.

Figure 5: Experimental setup for liquid crystal evaluation tests.

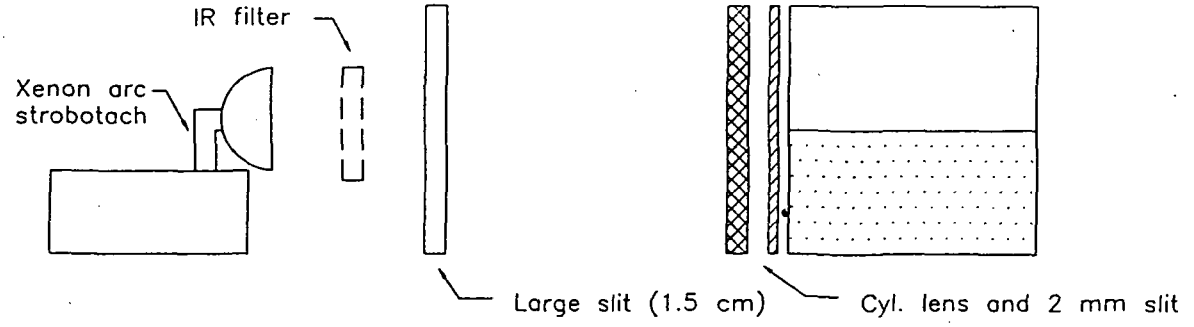

(d)

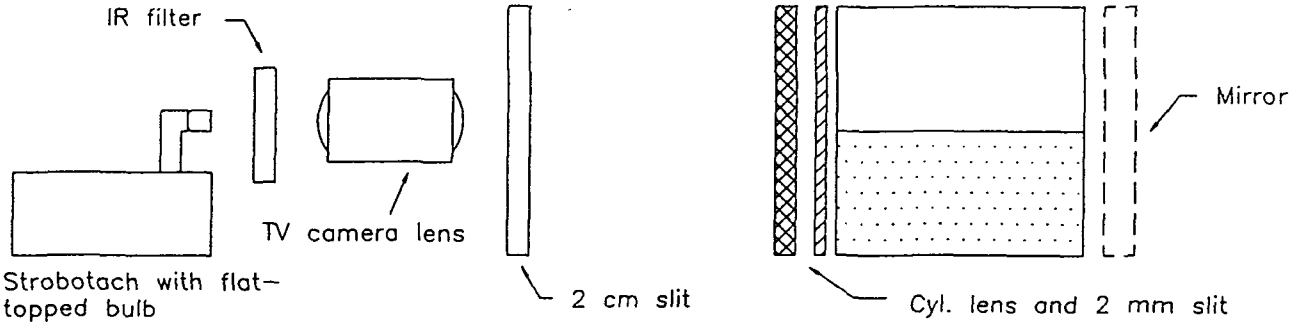

(e)

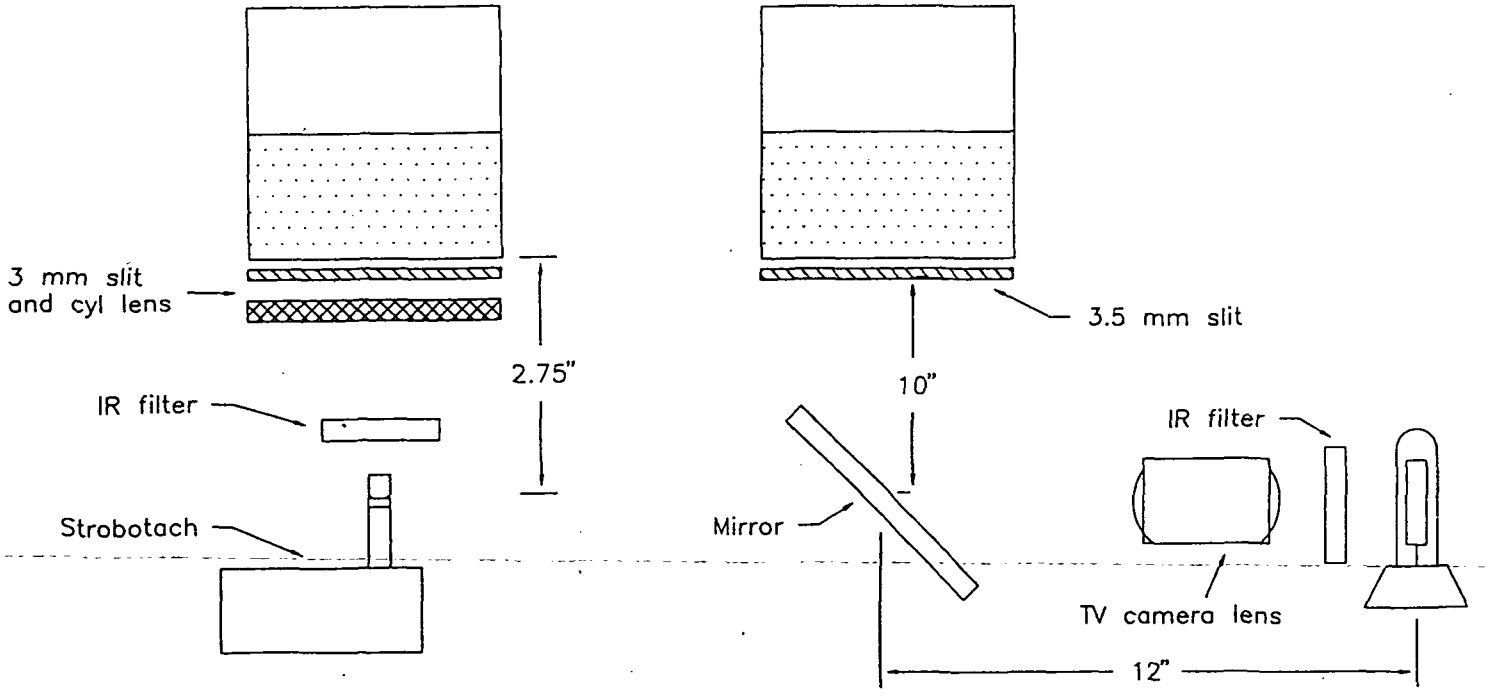

(f) (g)

Figure 5: Experimental setup for liquid crystal evaluation tests.

Appendix A.1: Data Summary: Single-Phase Tests

Run #	Tape #	Start time	Heater Size,cm	Heater Temp F	Order of flow pattern devel.	Stop time	Foot-notes	Comments
88 *	6	00:00	1.25	379	B,E	06:00	1,3	
89	6	06:00	1.25	342	C,E	13:14	3,4	
90	6	13:15	1.25	275		20:21	2,4	
91	6	20:22	1.25	326	C	27:38	4	
92	6	27:39	1.25	310		34:17	2,4	
93	6	34:18	1.25	430	C	40:06	3,4	
94	6	40:07	1.25	512	C	46:15	5	I
95	6	46:16	1.25	536	C	51:58	5,6	I
96	6	51:59	1.25	726	B,H	57:47	2,4	II
97	6	57:48	1.25	725	C,H	1:04:11	5	I
98	6	1:04:12	1.25	728	C,H	1:10:52	5,6	I
99	6	1:10:53	1.25	-	C,H	1:14:33	3,4	III
100	6	1:14:34	1.25	-	C,H	1:19:17	3,4,1	III
101	6	1:19:18	1.25	970	C,H,J	1:24:56	3	II
102	6	1:24:57	1.25	-	C,	1:29:22	1,3	III
103	6	1:29:23	1.25	978	C,H,J	1:35:47	3	IV
104	6	1:35:48	1.25	980	C,H,J	1:40:57	5,6	II
105	6	1:40:58	1.25	974	C,H,J	1:46:34	1,5	IV
106	6	1:46:35	1.25	968	C,H,J	1:52:59	3	II
107	6	1:53:00	1.25	971	C,H,J(?)	1:55:52	3,4	V
108	7	00:00	1.25	982	C,H,J	05:51	2,5	IV
109	7	05:52	1.25	979	C,H,J	11:11	3,4	II,V
110	7	11:12	1.25	967	C,H,	16:55	2,5,6	V
111	7	16:56	1.25	-		22:38	2	III
112	7		-	-				IX
113	7	23:06	1.25	950	C,H,J	28:46	5,6	I,IV
114	7	28:47	1.25	949	C,H,J	34:28	5,6	IV
115	7	34:29	1.25	950	C,H,J	40:00	5	IV
116	7	40:01	1.25	1019	C,H,J	45:07	1,4	IV
117	7	45:08	1.25	-		48:07		III
118	7	48:08	1.25	-		51:51		III
119	7	51:52	1.25	-		56:30		III
120	7	56:31	1.25	963	C,I	1:03:00	1,3,4	II,IV
121	7	1:03:01	1.25	985	C,	1:09:04	2,3,4	V
122	7	1:09:05	1.25	1002	C,I	1:16:50		II,IV
123	7	1:16:51	1.25	1033	C,H,J	1:21:25	5,6	III,IV
124	7	1;21:26	1.25	1024	C,H,J	1:28:30	5	IV
125	7	1:28:31	1.25	1027	C,H,J	1:32:58	5	III,IV
126	7	1:32:59	1.25	731	C,H	1:39:27	5	
127	7	1:39:28	1.25	-		1:43:52	1,3	VI
128	7	1:43:53	1.25	785	C,H	1:50:33	4	
129	7	1:50:34	1.25	767	C,H	1:57:07	4	
130	7	1:57:08	1.25	731	C,H	2:00:00	4	
131	8	00:00	1.25	720	C,H	07:07		
132	8	07:08	1.25	312	C,	13:01	1,3	V
133	8	13:02	1.25	322	C	19:20	4	
134	8		1.25	-				IX

* Note: Runs 1 through 87 are summarized in "An Investigation into the Flow Behavior of a Single-Phase Gas System in a Heated Enclosure Under Normal Gravity Conditions", Summer Faculty Fellow Report by Dr. Peter J. Disimile, September 1988.

Run #	Tape #	Start time	Heater Size,cm	Heater Temp F	Order of flow pattern devel.	Stop time	Foot-notes	Comments
135	8	25:17	1.25	985	C,K,J	33:34	5	IV,VII
136	8	33:35	1.25	986	C,J	40:00	1,3,4	VI,VII
137	8	40:01	1.25	998	C,K,J	48:34	5	IV,VII
138	8	48:35	1.25	1020	C,K,J	55:38	5	IV,VII
139	8	55:39	1.25	1033	C,K,	1:02:35	4	V,VII
140	8	1:02:36	1.25	992	C,K,J	1:11:04	4	IV,V,VII
141	8	1:11:05	1.25	985	C,	1:16:41	3,4	V,VII
142	8	1:16:42	1.25	1013	C,	1:24:31	3,4	V,VII
143	8	1:24:32	1.25	1007	C,K,	1:31:23	5	VII
144	8	1:31:24	1.25	1027	C,	1:39:50		VII,VIII
145	8	1:39:51	1.25	955	C,K,	1:44:54	4	V,VII,VIII
146	8	1:44:55	1.25	1030	C,K,	1:53:11	4	VII,VIII
147	8	1:53:12	1.25	1027	C,K,J	2:00:00	1,5	IV,VII
148	9	00:00	1.25	1005	C,K,J	06:58	5	IV,VII
149	9	06:59	1.25	1019		11:05	3	V,VI,VII
150	9	11:06	1.25	1024	C,K,	18:39		V,VII
151	9	18:40	1.25			31:46		III
152	9	31:47	1.25	1018	C,K,	39:45		V,VII
153	9	39:46	1.25	987	C,H,J	47:38	2	VI,VII
154	9	47:39	1.25	1010	C,H,J	57:52	5	IV,VII
155	9	57:53	1.25	1006	C,H,J	1:07:03	5	IV,VII
156	9	1:07:04	1.25	966		1:09:43		VI,VII
157	9	1:09:44	1.25	958		1:13:31	1,3	VII
158	9	1:13:32	1.25	1028	C,K,H	1:21:01		VII
159	9	1:21:02	1.25	984	C,K,J	1:31:13		IV,VII
160	9	1:31:14	1.25	755	C,K	1:38:07	5,6	VII
161	9	1:38:08	1.25	756	C,K	1:44:13	5,6	VII
162	9	1:44:14	1.25	1045	C,K,	1:50:31	4,5,6	I,IV
163	9	1:50:32	1.25	1033	C,K,J	2:00:00	5,6	I,IV
164	10	00:00	1.25	1010	C,H,J	08:33	4,5	I,IV
165	10	08:34	1.25	915	C,H	15:40	5,6	
166	10	15:41	1.25	959	C,H,J	23:43	5,6	IV,V
167	10	23:44	1.25	933	C,H,J	31:52	2,5,6	IV
168	10	31:53	1.25	1028	C,K	38:42	4	
169	10	38:43	1.25	1013	C,K	45:17	4	V
170	10	45:18	1.25	998	C,K	52:06	4	V
171	10	52:07	1.25	952	C,H	58:22	4,6	II
172	10	58:33	1.25	941	C,H	1:06:44	2,4	
173	10	1:06:45	1.25	-	C,H	1:13:48	1,5,6	III
174	10	1:13:49	1.25	989	C,H,J	1:22:10	5,6	IV
175	10	1:22:11	1.25	981	C,H,J	1:29:32	4	IV
176	10	1:29:33	1.25	740	C,H	1:35:56		II
177	10	1:35:57	1.25	728	C,H	1:43:06	2	
178	10	1:43:07	1.25	745	C,H	1:49:50	5	
179	10	1:49:51	1.25	944	C,H,J	2:00:00	4	
180	11	00:00	1.25	963	C,H,	07:31	3,4	VI
181	11	07:32	1.25	1048	C,H,J	17:57	2,3,4	IV,V
182	11	17:58	2.5	642	K,	25:18	4	V,VII
183	11	25:19	2.5	701	K,H,J	34:21	4	IV,VII
184	11	34:22	2.5	715	K,	44:26	3	II,VII
185	11	44:27	2.5	799		50:35	1,3,4	II,VII
186	11	50:36	2.5	768	K,	58:32	4	II,VII
187	11		2.5	-				IX
188	11	58:40	2.5	837	K,H,J	1:05:00	1,4	IV
189	11	1:05:01	2.5	695	K	1:11:29	4,5	V
190	11	1:11:30	2.5	813	C,H,J	1:21:48	5,6	I,IV

Run #	Tape #	Start time	Heater Size,cm	Heater Temp F	Order of flow pattern devel.	Stop time	Foot-notes	Comments
191	11	1:21:49	2.5	863	C,K,	1:29:23	4	V
192	11	1:29:24	2.5	914	C,K,H,J	1:38:50	4	
193	11	1:38:51	2.5	811	C,H,J	1:49:20	4	I,IV
194	11	1:49:21	2.5	827	C,K,J	2:00:00	4	
195	12	00:00	2.5	916	C,K,J	10:10	4	
196	12	10:11	2.5	910	C,K,J	17:23	4	V
197	12	17:24	2.5	906	C,	26:09	3,4	VI
198	12	26:10	2.5	-		28:28	6	IX
199	12	28:29	2.5	904	C,J	37:17	4	V,VI
200	12	37:18	2.5	911	C,K,J	45:24	3	II
201	12	45:25	2.5	906	C,H,J	53:47	3,5	V
202	12	53:48	2.5	880	C,H,J	1:00:48	3,4,5	IV
203	12	1:00:49	2.5	903	C,H,J	1:10:11	2,5	IV
204	12	1:10:12	2.5	892		1:18:56	3	IX
205	12	1:18:57	2.5	913		1:26:48	4	IX
206	12	1:26:49	2.5	334	C	1:35:30	4	V
207	12	1:35:31	2.5	331	C	1:42:20	3,4,6	
208	12	1:42:21	2.5	290	C	1:59:18	5,6	
209	12	1:59:19	2.5	330		2:00:00		VI
210	13	00:00	2.5	340		09:12	3,4	VI
211	13	09:13	2.5	-		12:21		VI
212	13	12:22	2.5	340		20:26		VI
213	13	20:27	2.5	331		27:41		VI
214	13	27:42	2.5	345	C	35:33	3,5	
215	13	35:34	2.5	344	C	43:00	5	
216	13	43:01	2.5	607	C,H,J	53:42	5	IV,VI
217	13	53:43	2.5	531	C,H	1:02:06	1,3,4	
218	13	1:02:07	2.5	-		1:06:45	3,4	
219	13	1:06:46	2.5	511	C,H	1:14:29	3,5,6	
220	13	1:14:30	2.5	500	C,H	1:22:13	3,5,6	
221	13	1:22:14	2.5	661	C,H,	1:29:34	4	II
222	13	1:29:35	2.5	725	C,H,J	1:37:49	4,5	IV
223	13	1:37:50	2.5	731	C,H,J	1:45:23	3,5	I,IV
224	13	1:45:24	2.5	737	C,H,	1:53:58	3,4	
225	13	1:53:59	2.5	743	C,H,J	2:00:00	5,6	I,IV
226	14	00:00	2.5	-		04:51	3,4	
227	14	04:52	2.5	848	C,H,J	11:20	3,4	II,IV
228	14	11:21	2.5	842	C,H,J	19:32	3,5	I,IV
229	14	19:33	2.5	931	C,H,J	27:10	2,3,5	IV
230	14	27:11	2.5	850	C,H,	31:41	3,4	II
231	14	31:42	2.5	957	C,H,J	39:21	4	IV,V
232	14	39:22	2.5	948	C,H,J	46:28	2,4	IV
233	14	46;29	2.5	946	C,H,J	53:50	2,5,6	V
234	14	53:51	2.5	996	C,K,J	58:46	3,4	IV,VII
235	14	58:47	2.5	999	C,H,	1:01:14	3,4	V,VII
236	14	1:01:15	2.5	994	C,K,J	1:06:37	3,5	IV,VII
237	14	1:06:38	2.5	985	C,K,J	1:12:02	2,3,5	IV,VII
238	14	1:12:03	2.5	975	C,K,J	1:19:22	3,5	IV,VII
239	14	1:19:23	2.5	970	C,K,J	1:25:12	3,5	IV,VII
240	14	1:25:13	2.5	972	C,K,	1:29:54	3,4	V,VII
241	14	1:29:55	2.5	973	C,H,J	1:36:08	2,3	IV
242	14	1:36:09	2.5	977	C,K,J	1:47:39	3,4	VII
243	14	1:47:40	2.5	953	C,K,J	1:53:42	3,4	VII
244	14	1:53:43	2.5	722	C,H	2:00:00	3,4	VII
245	15	00:00	2.5	734	C,K	06:00	3,4,5,6	VII
246	15	06:01	2.5	1030	C,H,J	14:13	2,6	I,IV
247	15	14:14	2.5	1028	C,H,J	22:02	3,5	I,IV

Footnotes:

1. Smoke too faint for adequate visualization.
2. Smoke too dense, lost contrast.
3. Some circulation in test cell prior to energizing heater.
4. Flow out of plane of visualization.
5. Good symmetry
6. Good roll-up

Comments:

I. Good clarity.
II. Asymmetric flow patterns.
III. Run stopped early due to too high a heater temperature or equipment failure.
IV. Lower vortical cell clearly forms.
V. Poor clarity.
VI. Large circulation present at start of run.
VII. Heater near steady state temperature before being placed on the test cell.
VIII. Experienced problems with heater, power reduced soon after beginning of run.
IX. Run not recorded or recorded over.

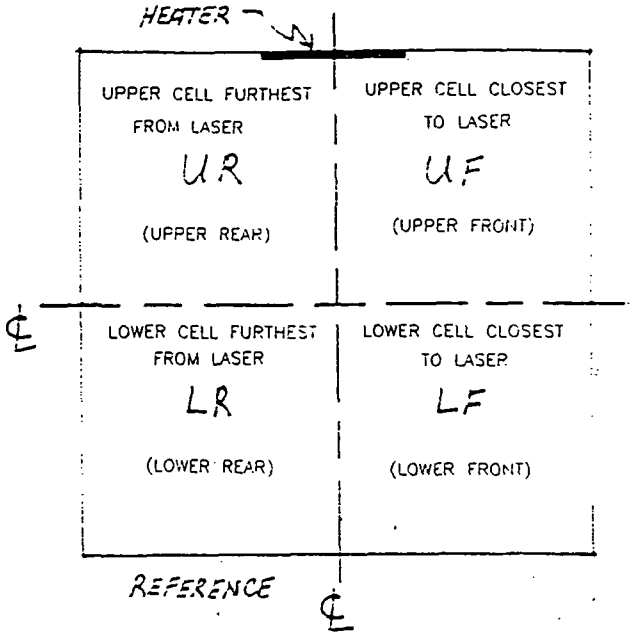
HEATER
UPPER CELL FURTHEST FROM LASER
UR
(UPPER REAR)
UPPER CELL CLOSEST TO LASER
UF
(UPPER FRONT)
LOWER CELL FURTHEST FROM LASER
LR
(LOWER REAR)
LOWER CELL CLOSEST TO LASER
LF
(LOWER FRONT)
REFERENCE

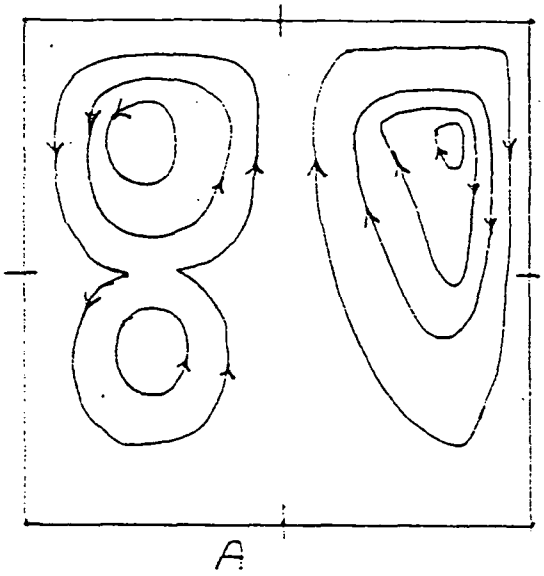
A

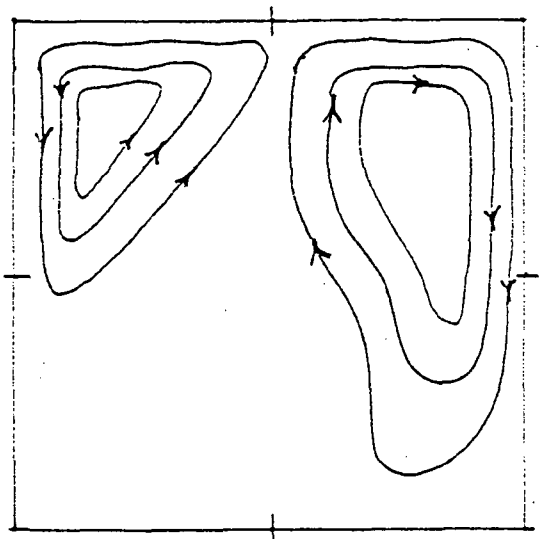
B

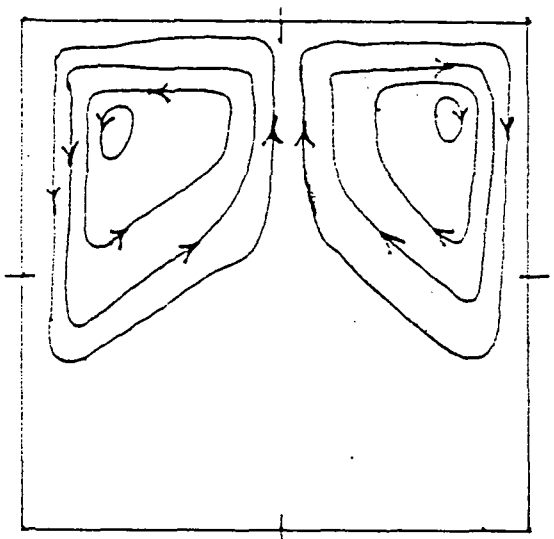
C

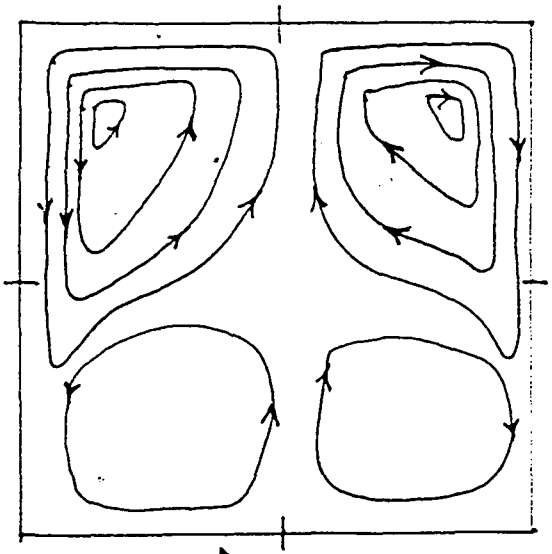
D

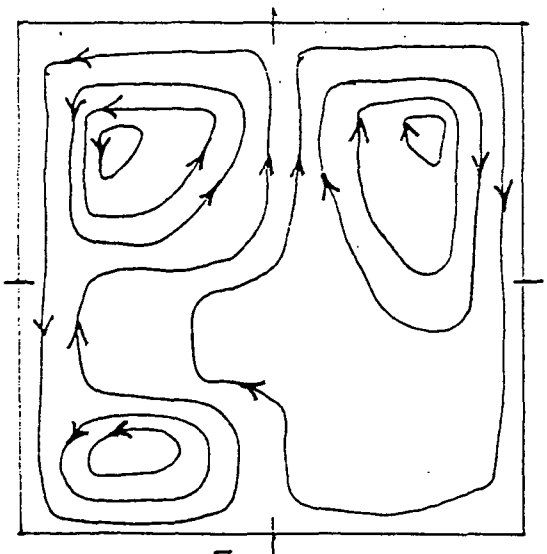
E

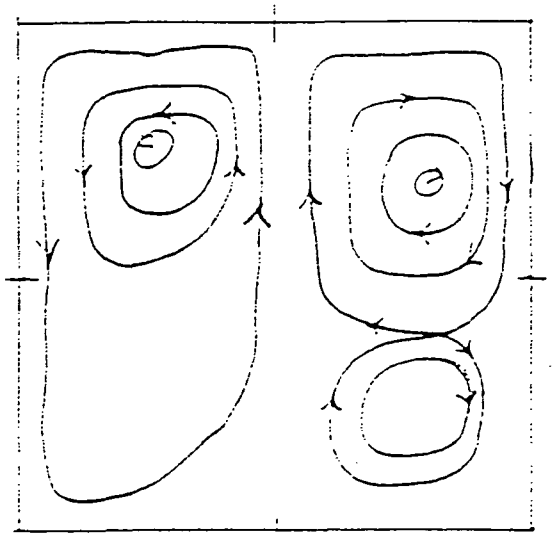

F

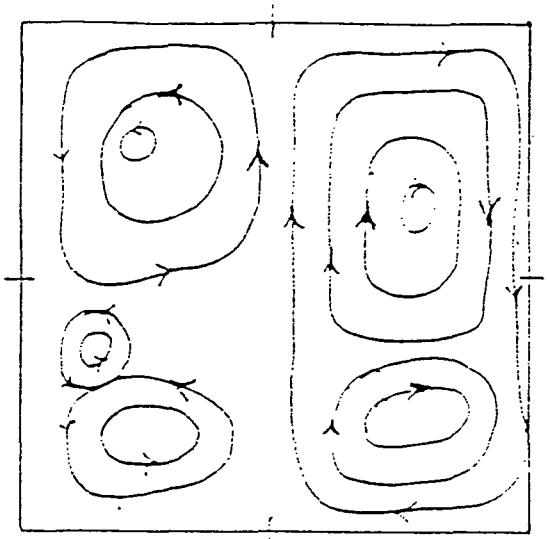

G

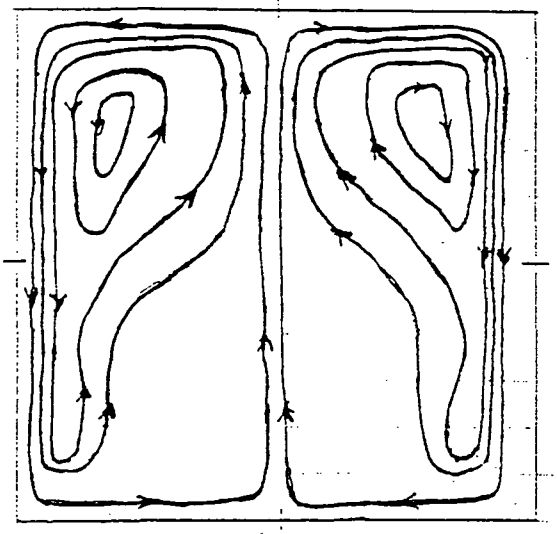

H

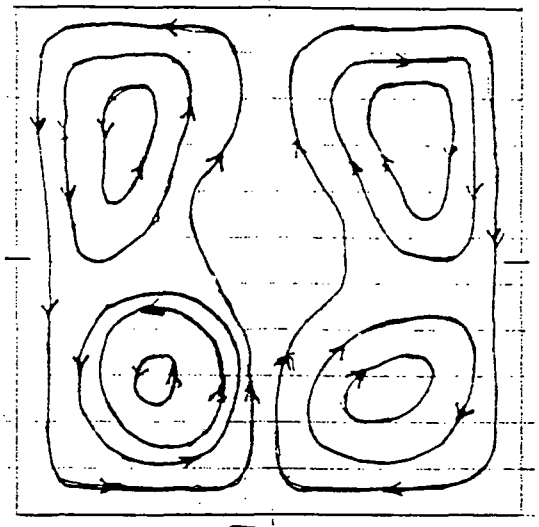

I

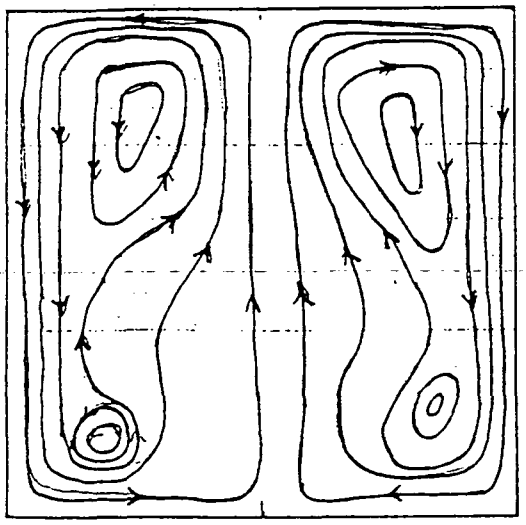

J

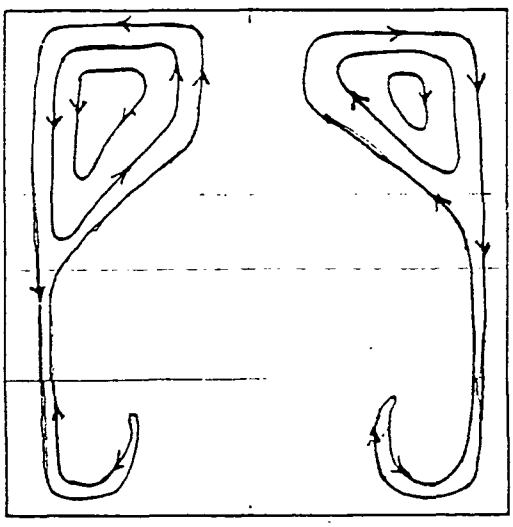

K

Appendix A.2: Data Summary: Two-Phase Tests

Run #	Tape #	Start count	Stop count	Test cell size, HxD (cm)	Heater Size, cm	Heater Temp, F	Comments
1	1	0	479	10 x 5	1.25	974	
2	1	480	1078	10 x 5	1.25	994	1
3	1	1079	1529	10 x 5	1.25	1000	
4	1	1530	1910	10 x 5	1.25	980	
5	1	1911	2325	10 x 5	1.25	980	2
6	1	2326	2746	10 x 5	1.25	980	
7	1	2747	3010	10 x 5	1.25	538	3
8	1	3011	3330	10 x 5	1.25	680	4
9	1	3331	3635	10 x 5	1.25	785	
10	1	3636	3904	10 x 5	1.25	720	
11	1	3905	4196	10 x 5	1.25	724	
12	1	4197	4440	10 x 5	1.25	578	5
13	1	4441	4663	10 x 5	1.25	577	
14	1	4664	4860	10 x 5	1.25	222	3
15	1	4861	5035	10 x 5	1.25	202	
16	1	5036	5326	10 x 5	2.5	480	2
17	1	5327	5616	10 x 5	2.5	667	
18	1	5617	end	10 x 5	2.5	1000	
19	2	0	422	10 x 5	2.5	820	
20	2	423	852	10 x 5	2.5	1015	
21	2	853	1312	10 x 5	2.5	993	
22	2	1313	1732	10 x 5	2.5	755	
23	2	1733	2220	10 x 5	2.5	760	6,8
25 *	2	3113	3410	10 x 5	2.5	757	6
26	2	3411	3735	10 x 5	2.5	738	6,8,9
27	2	3736	4135	10 x 5	2.5	745	6,8,9
28	2	4136	4482	10 x 5	2.5	746	6,9
29	2	4483	4751	10 x 5	2.5	758	6,8,9,10
30	2	3732	4057	10 x 5	2.5	756	7,9,11
31	2	4058	4405	10 x 5	2.5	699	7,9
32	2	4406	4590	10 x 5	2.5	984	7,9,11
33	2	4591	4877	10 x 5	2.5	770	7,9
34	2	4878	5129	10 x 5	1.75	698	12
35	2	5130	5378	10 x 5	1.75	753	
36	2	5379	5639	10 x 5	1.75	757	
37	2	5640	end	10 x 5	1.75	982	
38	3	0	448	10 x 5	1.75	985	
39	3	449	811	10 x 5	1.75	988	
40	3	812	1213	10 x 5	1.75	580	
41	3	1214	1549	10 x 5	1.75	582	
42	3	1550	1945	10 x 5	1.75	988	6,8
43	3	1550	1934	10 x 5	1.75	580	7,9
44	3	1935	2379	10 x 5	1.75	578	7,9
45	3	1946	2392	10 x 5	1.75	751	6,9
46	3	2383	2771	10 x 5	1.75	739	7,9
47	3	2772	3231	10 x 5	1.75	748	7,8,9
48	3	2392	2775	10 x 5	1.75	743	6,8
49	3	2776	3121	10 x 5	1.75	748	6,8
50	3	3122	3414	10 x 5	1.75	976	6,8,9
51	3	3415	3681	10 x 5	1.75	976	6,8
52	3	3232	3548	10 x 5	1.25	991	7
53	3	3549	3789	10 x 5	1.25	994	7
54	3	3850	4155	5 x 5	1.75	970	7,13

* Run 24 does not exist.

Run #	Tape #	Start count	Stop count	Test cell size, HxD (cm)	Heater Size, cm	Heater Temp, F	Comments
55	3	4156	4400	5 x 5	1.75	978	7,13
56	3	4401	end	5 x 5	1.75	750	7,13
56b	4	0	320	5 x 5	1.75	750	13,14
57	4	321	640	5 x 5	1.75	980	13,14
58	4	641	1482	5 x 5	1.75	750	13
59	4	1483	1900	5 x 5	1.75	587	13
60	4	1901	2266	5 x 5	1.75	578	13
61	4	2267	2564	5 x 5	1.75	970	13
62	4	2565	2874	5 x 5	1.75	970	15
63	4	2875	3200	5 x 5	1.75	750	15
64	4	3201	3498	5 x 5	1.75	580	15
65	4	3499	3774	5 x 5	1.25	560	15
66	4	3775	4058	5 x 5	1.25	730	15
67	4	4059	4301	5 x 5	1.25	979	15
68	4	4302	4529	5 x 5	1.25	975	15
69	4	4530	5140	5 x 5	1.25	978	15
70	4	5141	5781	10 x 10	1.75	972	8
71	4	5782	end	10 x 10	1.75	972	8
72	5	0	559	10 x 10	1.75	752	8
73	5	560	906	10 x 10	1.75	581	8
74	5	907	1317	10 x 10	1.25	680	8
75	5	1318	1672	10 x 10	1.25	975	8
76	5	1673	2032	10 x 10	1.25	770	8
77	5	2033	2385	10 x 10	1.25	568	8
78	5	2386	2815	10 x 10	1.75	980	8
79	5	2816	3332	10 x 10	1.75	760	8
80	5	3333	3874	10 x 10	1.75	570	8
81	5	3875	4399	10 x 10	1.25	970	
82	5	4400	4789	10 x 10	1.25	970	8
83	5	4790	5229	10 x 10	1.25	730	8

Comments :

1. Dark streaks in liquid outlining vorticies
2. Vorticies in liquid very clearly defined
3. Little or no noticeable liquid motion at the interface
4. Motion at interface and return motion clearly visible
5. Very slow liquid motion at interface
6. Rig camera only
7. Interface camera only
8. 35 mm camera used for long exposure pictures at interface. See lab book for details.
9. Gas phase tracer (tobacco smoke) used, smoke particles entrained in liquid clearly outline vorticies.
10. Silicone oil becoming cloudy from smoke contamination, difficult to detect liquid motion.
11. Heater inserted after reaching steady state temperature
12. New silicone oil
13. 5 x 5 cm square test cell, inner diameter actually 4.2 cm
14. Single phase test (gas only)
15. 5 x 5 cm round test cell

Appendix A.3: Data summary: Liquid crystal evaluation tests

Run #	Roll #	Film speed	Heater size, cm	Heater temp., F	Lighting method *	Comments
1	1	ASA 100	1.25	-	A	
2	2	ASA 100	1.25	910	B	
3	3	ASA 100	1.25	780	B	
4	3	ASA 100	1.25	600	B	
5	4	ASA 100	1.25	580	B	
6	5	ASA 100	1.75	560	C	
7	5	ASA 100	1.75	940	C	
8	5	ASA 100	1.75	570	C	2
9	5	ASA 100	1.75	730	C	2,3
10	6	ASA 400	1.75	965	C	2,3
11	6	ASA 400	1.75	965	C	2,3
12	7	ASA 1000	1.75	730	C	2,3,4
13	7	ASA 1000	1.75	980	B	1,2,4
15 **	8	ASA 400	1.75	940	B	2
16	8	ASA 400	1.75	850	D	
17	8	ASA 400	1.75	980	D	
18	9	ASA 1000	1.75	-	D	5
19	9	ASA 1000	1.75	-	D	5
20	9	ASA 1000	1.75	-	D	1,5
21	10	ASA 400	1.25	920	D	6
22	10	ASA 400	1.25	980	D	1,6
23	11	ASA 1000	1.75	980	D	4
24	11	ASA 1000	1:75	980	D	4
25	12	ASA 400	1.75	950	D	6
26	12	ASA 400	1.75	740	D	6
27	12	ASA 400	1.75	980	D	6,7
28	13	ASA 400	1.75	-	D	4,6,8
29	13	ASA 400	1.75	-	D	4,6,8
30	13	ASA 400	1.25	-	D	4,6,8
31	14	ASA 400	1.25	760	D	6,7,8
32	14	ASA 400	1.25	940	D	6,7,8
33	14	ASA 400	1.25	940	B	1,6,8,9
34	15	ASA 400	1.25	970	B	1,6,9
35	15	ASA 400	1.25	970	B	1,6,9
36	16	ASA 400	1.25	750	E	6
37	16	ASA 400	1.25	750	E	6
38	17	ASA 400	1.25	750	E	6
39	17	ASA 400	1.25	945	E	6
40	18	ASA 400	1.25	750	E	6,10
41	18	ASA 400	1.25	750	E	6,10
42	19	ASA 400	1.25	970	E	10,11
43	19	ASA 400	1.25	970	E	11
44	20	ASA 1000	1.25	840	E	11,13
45	20	ASA 1000	1.25	915	E	11,13
46	20	ASA 1000	1.25	950	E	7,11,13
47	21	ASA 3200	1.25	940	E	11,13
48	22	ASA 1000	1.25	980	E	6,13

* The various lighting methods are shown in Figure 4.

** Run 14 does not exist.

Run #	Roll #	Film speed	Heater size, cm	Heater temp., F	Lighting method	Comments
49	22	ASA 1000	1.25	980	E	6,7,13
49b	23	ASA 1000	1.25	940	E	6,13
50	23	ASA 1000	1.25	940	E	6,7,13
51	24	ASA 400	1.25	965	F	12
52	24	ASA 400	1.25	965	F	1,12
53	25	ASA 400	1.25	975	F	1,14
54	26	ASA 400	1.25	975	F	1,14
55	27	ASA 400	1.25	980	G	14
56	28	ASA 400	1.25	980	G	14
57	29	ASA 400	2.5	970	G	14
58	30	ASA 400	2.5	980	G	15

Comments :

1. IR filter included
2. Heat trap included
3. Fan included
4. Very poor picture quality
5. Camera malfunction, film not exposed
6. 1 cc TLC concentrate mixture
7. Strobotach flash rate increased to 300-325 rpm range
8. Ektachrome slide film used
9. Series of slits (2 cm, 5mm) placed in front of test cell and cyl. lens. Attempted to intermittently block lamp to reduce light induced motion.
10. Mirror in place
11. 4 cc TLC concentrate mixture
12. 10 cc TLC concentrate mixture
13. AFGA slide film used
14. 10 x 10 test cell with 45 cc concentrate mixture
15. 10 x 10 test cell with 500 m TLC particles

NASA
National Aeronautics and Space Administration

Report Documentation Page

1. Report No.	2. Government Accession No.	3. Recipient's Catalog No.
NASA CR-185304		

4. Title and Subtitle

An Investigation into the Flow Behavior of a Single Phase Gas System and a Two Phase Gas/Liquid System in Normal Gravity with Nonuniform Heating from Above

5. Report Date

October 1989

6. Performing Organization Code

7. Author(s)

Peter J. Disimile and Timothy J. Heist

8. Performing Organization Report No.

None

10. Work Unit No.

674-22-05

9. Performing Organization Name and Address

University of Cincinnati
College of Engineering
Cincinnati, Ohio

11. Contract or Grant No.

NAG3-938

13. Type of Report and Period Covered

Contractor Report
Final

12. Sponsoring Agency Name and Address

National Aeronautics and Space Administration
Lewis Research Center
Cleveland, Ohio 44135-3191

14. Sponsoring Agency Code

15. Supplementary Notes

Project Manager, Howard Ross, Space Experiments Division, NASA Lewis Research Center.

16. Abstract

The fluid behavior in normal gravity of a single phase gas system and a two-phase gas/liquid system in an enclosed circular cylinder heated suddenly and nonuniformly from above has been investigated. Flow visualization was used to obtain qualitative data on both systems. The use of thermochromatic liquid crystal particles as liquid phase flow tracers was evaluated as a possible means of simultaneously gathering both flow pattern and temperature gradient data for the two-phase system. The results of the flow visualization experiments performed on both systems can be used to gain a better understanding of the behavior of the such systems in a reduced gravity environment and aid in the verification of a numerical model of the system.

17. Key Words (Suggested by Author(s))	18. Distribution Statement
Buoyancy Thermocapillary flow	Unclassified – Unlimited Subject Category 29

19. Security Classif. (of this report)	20. Security Classif. (of this page)	21. No. of pages	22. Price*
Unclassified	Unclassified	32	A03

NASA FORM 1626 OCT 86

*For sale by the National Technical Information Service, Springfield, Virginia 22161